ACS OMEGA

Open Access

http://pubs.acs.org/journal/acsodf

Article

Achieving a Porous PDMS Film for Passive Cooling through the Utilization of Ultrafine NaCl Sacrificial Templates

Hongmei Zhong,* Ting Meng, Wenxiang Ding, Yi Xiao, and Peng Zhang*

Cite This: *ACS Omega* 2025, 10, 1012−1018

Read Online

ACCESS | Metrics & More | Article Recommendations | Supporting Information

ABSTRACT: Passive radiative cooling technology serves as an energy-free alternative to traditional cooling systems. Porous polymer structures are frequently employed for radiative cooling by leveraging the refractive index mismatch between the polymer and the pores, enabling the scattering of incoming sunlight. Recently, water-soluble and readily available Sodium chloride (NaCl) particles have been utilized as sacrificial templates for sustainable pore creation. Nevertheless, optimizing NaCl particle size, and thus the polymer pore size to enhance scattering capabilities remains a challenge. Here, we report a simple, scalable, and sustainable approach to creating an optimized porous polydimethylsiloxane (PDMS) film. This approach utilizes ultrafine NaCl powders as sacrificial templates, which were synthesized via ultrasonic precipitation to ensure their small size. The ultrafine NaCl particles have a size distribution centered around 6−8 μm, and the as-fabricated porous PDMS film achieves a high thermal emissivity of 0.95 within the atmospheric window (8−13 μm) and exhibits a reflectivity of 0.95 within the visible range (0.4−0.78 μm). Due to the desired dual-spectrum properties, the porous PDMS film exhibits a superior subambient cooling capacity over that fabricated with typically larger NaCl particles under strong sunlight. This study offers a scalable and practical radiative cooling solution for sustainable thermal management.

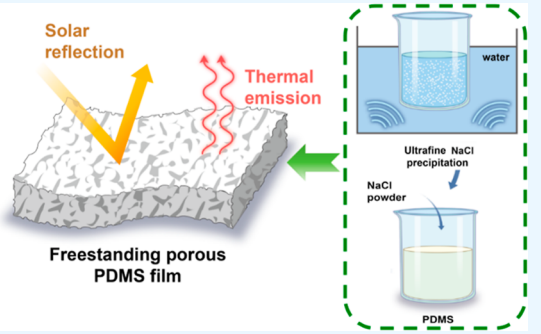

INTRODUCTION

The utilization of compressor-based cooling systems is contributing to the exacerbation of global warming.[1] Considering the principle of sustainable development, there is a critical necessity to explore passive cooling alternatives. Radiative cooling, which capitalizes on the cold temperature of the universe for radiative heat dissipation, has been increasingly recognized as a viable solution and has experienced notable progress.[2] This approach entails the utilization of materials and structures with specific optical properties, such as high solar reflectance (0.3−2.5 μm) and strong infrared (IR) emission (within the atmospheric transparent window of 8−13 μm).[3] Various materials and structures have demonstrated effective cooling capabilities, including multilayer photonic structures,[4] hybrid optical metamaterials,[5] hierarchically fibrous materials,[6] and porous polymer structures.[7]

In recent years, there has been a growing focus on developing radiative cooling materials at a larger scale. Therefore, progress has shifted from dedicated photonic structures and metamaterials to scalable porous materials.[8−16] The effectiveness of porous materials in radiative cooling relies on the high solar reflection through Mie scattering, influenced by the refractive index transition across polymer−air boundaries.[17] This scattering mechanism becomes more noticeable as the pore size approaches the target wavelength. Various techniques, including the phase inversion method,[18,19] electrospinning method,[20,21] and medium embedding-extracting method,[22,23] have been employed to fabricate hierarchically porous polymer materials. Nevertheless, these approaches frequently entail intricate preparation procedures utilizing solvents or particles that may pose risks to human health or the environment. To avoid the risks, readily available and eco-friendly NaCl particles have been recently utilized as sacrificial templates for pore formation.[24−28] However, it remains a challenge to attain smaller-size NaCl particles to optimize the optical properties of the resulting porous structures.

Herein we propose an approach to fabricate porous polydimethylsiloxane (PDMS) films for radiative cooling using ultrafine NaCl particles as sacrificial templates, where the small-size NaCl particles were prepared by precipitation under continuous sonication. The porous structure of the PDMS allows efficient sunlight reflection, which reduces solar heat gain. Additionally, the intrinsic molecular vibrations of PDMS polymer provide a high mid-infrared emittance, which expedites radiative heat dissipation through the atmospheric

Received: September 9, 2024
Revised: December 18, 2024
Accepted: December 19, 2024
Published: December 27, 2024

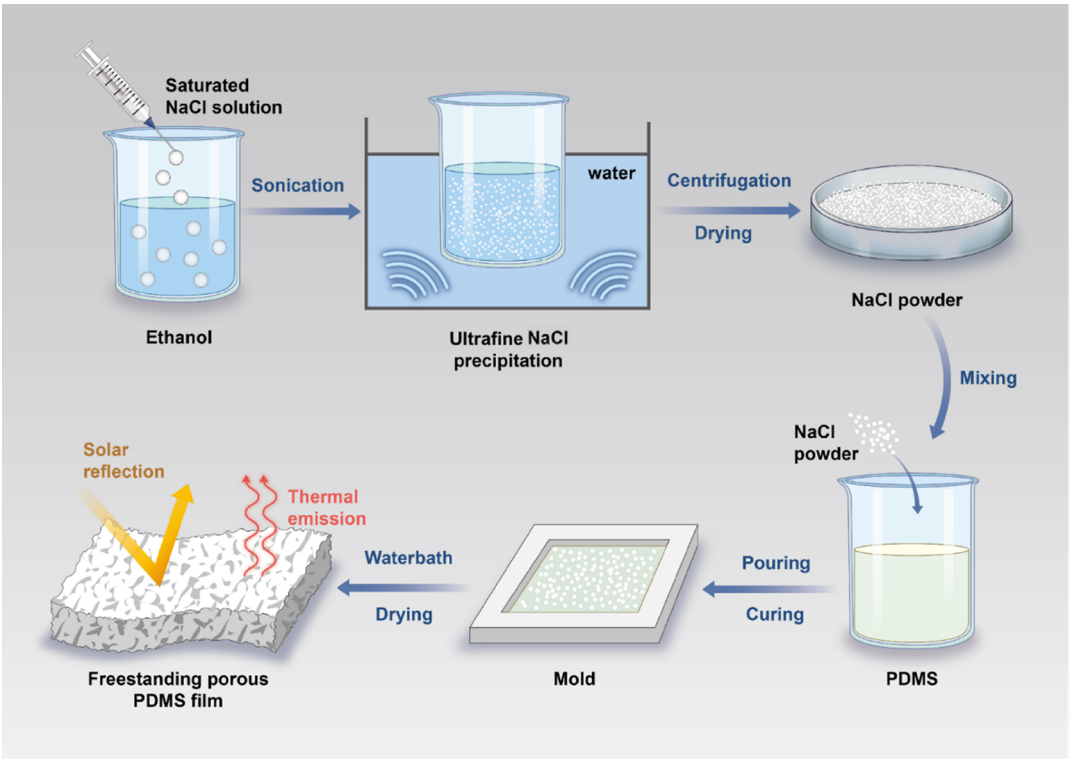

Figure 1. Schematic illustrating the preparation of the porous PDMS film using ultrafine NaCl sacrificial templates. The NaCl templates are prepared through ultrasonic precipitation.

window. Consequently, the porous PDMS film demonstrates desirable properties for radiative cooling, with a high reflectivity of 0.95 in the visible region (0.4−0.78 μm) and an emissivity of 0.95 in the 8−13 μm wavelength range. Field tests of the porous PDMS film demonstrated a 7 °C drop in air temperature under direct sunlight, showing superior sub-ambient cooling compared to the film fabricated using typical larger NaCl particles.

RESULTS AND DISCUSSION

We present a simple, scalable, and sustainable fabrication approach that employs ultrafine NaCl sacrificial templates to create porous structures for radiative cooling. The ultrafine NaCl powders are synthesized through a precipitation method assisted by ultrasonication to guarantee their small size. As for the base material, we carefully selected PDMS due to its capacity to enable high broadband emission within the mid-infrared wavelength spectrum, facilitated via various molecular bond vibrations (such as Si−O−Si and C−H).[29]

The general fabrication procedure is shown in Figure 1. The first step is the synthesis of ultrafine NaCl powders by ultrasonic precipitation. Specifically, 5 mL of NaCl aqueous solution (3.0 M, J&K) was gradually added to 80 mL of ethanol (GR, Aladdin). Subsequently, the mixture underwent continuous sonication for 180 s (GT sonic P3, 30 W, 40 kHz). Following the reaction, the white ultrafine NaCl precipitates were gathered via centrifugation (1000 rpm, 2 min) and then dried in an oven at 80 °C for 24 h. We also prepared NaCl precipitates subjected to various sonication durations and subsequently acquired scanning electron microscopy (SEM) images of each sample. The results suggest that further extending the sonication time has minimal impact on particle size (Figure S1). For comparison, NaCl silent precipitates were prepared following the same procedure except for the introduction of sonication. Additionally, commercial NaCl powders (GR, 99.8%, Macklin) and cooking salt were procured as control samples.

The ultrafine NaCl powders synthesized by ultrasonic precipitation were then utilized as sacrificial templates to create a porous PDMS film (U−P−PDMS). The powders were poured into a beaker, followed by the addition of the premixed PDMS precursor (Sylgard 184, Dow Corning). The mass ratio of NaCl to PDMS was adjusted to 1:1 to ensure the proper dispersion of the ultrafine NaCl particles in the viscous PDMS precursor. After thorough mixing, the resulting mixture was transferred into a flat rectangular polytetrafluoroethylene mold to control the configuration and dimensions of the porous (PDMS) film, which were set to 5 cm × 5 cm × 1 mm. The mixture was subsequently cured at 80 °C for 3 h, detached from the mold, and immersed into a water bath at 75 °C for 12 h to remove the NaCl particles. Finally, the freestanding porous PDMS film was obtained after drying in a hot oven at 80 °C for 3 h to eliminate residual water. For comparison, samples of porous PDMS fabricated using different NaCl templates were prepared at the same mass ratio of 1:1 and the same size of 5 cm × 5 cm × 1 mm, including S−P−PDMS prepared with NaCl templates that were silently precipitated without sonication, M−P−PDMS prepared with commercial NaCl powders (GR, 99.8%, Macklin) and C−P−PDMS prepared with cooking salt.

As depicted in Figure 2A, the U−P−PDMS film prepared with the ultrafine NaCl templates exhibits excellent flexibility, and the whitest color appearance among all the samples, indicating the highest reflectivity across the visible light spectrum. The surface structure of the porous PDMS films was revealed by the SEM images (SEM, TESCAN MIRA

https://doi.org/10.1021/acsomega.4c08275
ACS Omega 2025, 10, 1012−1018

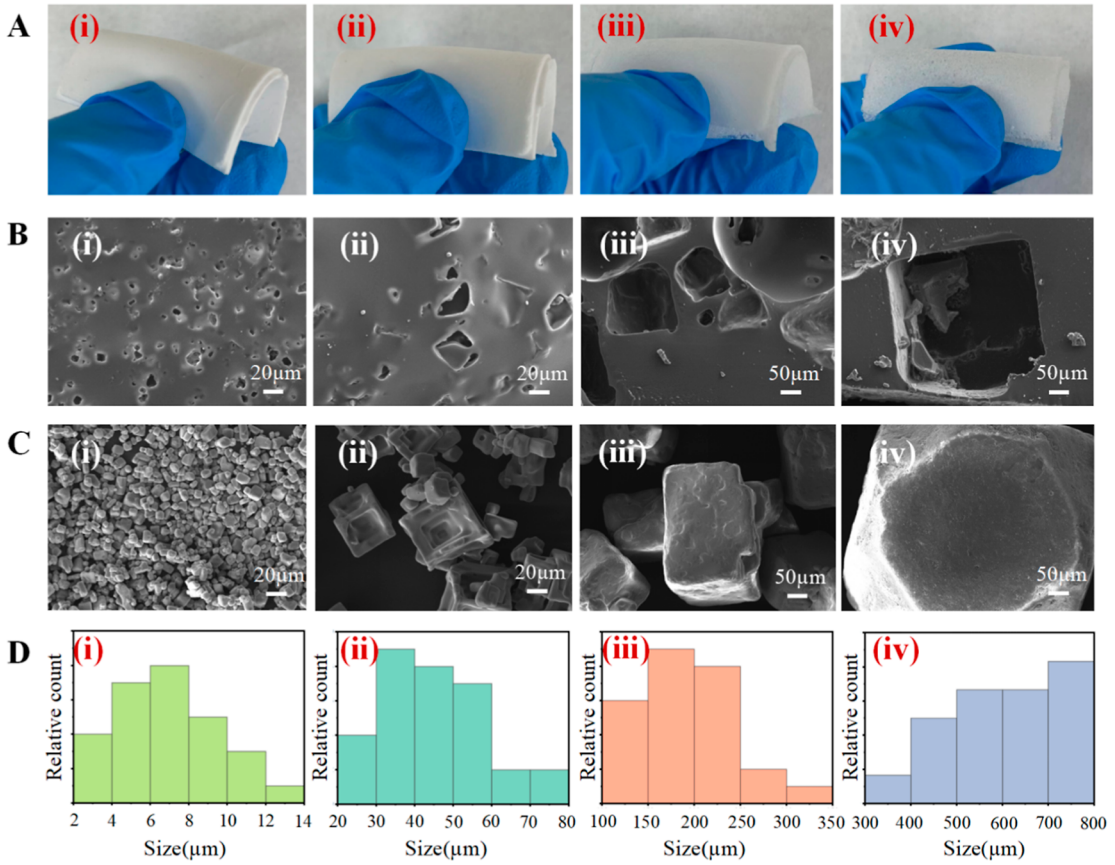

Figure 2. (A) Photographs showing the whiteness and flexibility of the (i) U−P−PDMS film prepared with ultrafine NaCl templates synthesized by ultrasonic precipitation, (ii) S−P−PDMS prepared with NaCl templates synthesized by silent precipitation without ultrasonication, (iii) M−P−PDMS prepared with commercial NaCl powders (GR, 99.8%, Macklin), (iv) C−P−PDMS prepared with cooking salt. (B) SEM images of the porous PDMS films. The sequence from (i−iv) corresponds to the order depicted in Figure 2A. (C) SEM images of (i) ultrafine NaCl templates synthesized by ultrasonic precipitation, (ii) NaCl templates synthesized by precipitation without sonication, (iii) commercial NaCl powders (GR, 99.8%, Macklin), (iv) cooking salt. (D) Size distribution of all the NaCl particles. The sequence from (i−iv) corresponds to the order depicted in Figure 2C.

LMS). As expected, NaCl templates indeed produce porous structures in PDMS films, and the U−P−PDMS showcases the most compact and smallest pore distribution (Figure 2B). The square-shaped micropores in all the samples are consistent with the size of NaCl templates. As shown in Figure 2C,D, ultrafine NaCl powders synthesized through ultrasonic precipitation have a size range centered around 6−8 μm, while those precipitated without sonication are around 40−50 μm. The formation of smaller NaCl crystals was attributed to the influence of ultrasonication on nucleation rate.[30,31] Increasing the parameters of ultrasonication, including frequency, power, and duration, generally leads to a decrease in particle size. However, prior research suggests that the effect is relatively modest, as the resulting NaCl particles rarely exhibit sizes below 1 μm.[32,33] Nevertheless, the NaCl particles formed from precipitation are smaller than procured commercial NaCl particles and cooking salt. Compared with the porous PDMS films fabricated using larger NaCl particles, the small pores in U−P−PDMS are promising to improve the optical scattering feature desired for solar absorption suppression.

Figure 3A shows that U−P−PDMS can achieve a high emissivity of 0.95 within the atmospheric window (8−13 μm) and reflectivity of 0.85 within the solar spectrum (0.3−2.5 μm) (PerkinElmer Lambda 950 UV/vis/NIR, Nicolet iS50 FTIR, replicated data can be found in Figure S2). Specifically, it exhibits a reflectivity of 0.95 within the visible range (0.4−0.78 μm), where most solar radiation is present. We also measured the spectra of porous PDMS samples fabricated by other NaCl templates and plotted the results in Figure 3B,C (replicated data can be found in Figures S3and S4). All porous PDMS exhibit higher solar reflectivity and infrared emissivity than pure PDMS, highlighting the role of porous structures in enhancing the optical properties for radiative cooling. In particular, porous PDMS films fabricated with smaller particle sizes show stronger solar reflection (Figure 3B). It is because the reduction in the size of NaCl particles leads to an increase in pore density and a corresponding decrease in pore size, which approaches the wavelength of the solar spectrum. This phenomenon enhances the efficiency of solar scattering. Notably, the solar reflectivity of U−P−PDMS surpasses that of M−P−PDMS-5:1 and C−P−PDMS-5:1, where the NaCl to PDMS ratio is increased to 5:1. This observation suggests that just a small concentration of ultrafine NaCl particles can achieve a better optical property for cooling. The emission spectra indicate that all five films exhibit strong thermal emittance within the atmospheric transparent window, attributable to the inherently high emissivity of the PDMS matrix (Figure 3C). However, the emissivity of the U−P−PDMS film surpasses that of the other four films, which can be

https://doi.org/10.1021/acsomega.4c08275
ACS Omega 2025, 10, 1012−1018

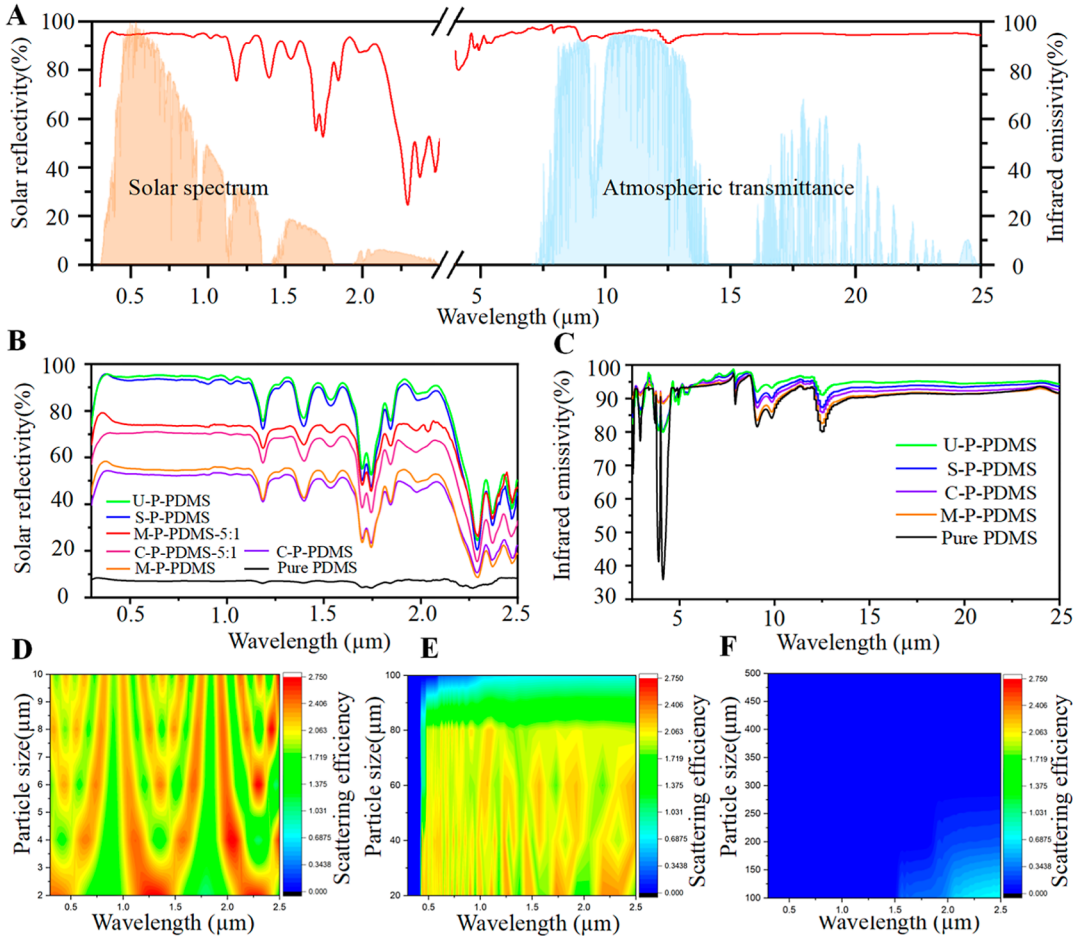

Figure 3. (A) Measured solar reflectivity and infrared emissivity of the U−P−PDMS, along with the solar spectrum and the atmospheric transparent window. (B) Comparison of measured solar reflectivity of U−P−PDMS with other samples. (C) Comparison of measured infrared emissivity of U−P−PDMS with other samples. (D−F) Simulated solar scattering efficiency of the porous PDMS film with different pore sizes.

ascribed to a more efficient gradual refractive index transition that increases air-medium interface absorption at mid-infrared regions.[34,35]

We performed scattering efficiency calculations for pores as a function of pore size across the solar spectrum. These calculations were based on Mie theory and conducted using Finite-difference time-domain (FDTD) simulations (Lumerical FDTD). Mie scattering occurs when electromagnetic waves interact with scatterers that are comparable in size to or larger than the wavelength of the waves.[22] We used a two-dimensional model to simplify analysis and reduce simulation time (Figure S5), simulating the scattering efficiency of various micropores at solar wavelengths from 0.25 to 2.5 μm. Perfect matching layer (PML) absorption boundary conditions and a total field scattered field (TFSF) source were employed. The results confirm that the pores with a size distribution between 6 and 8 μm can obtain a high scattering efficiency above 1.0 in the solar wavelength range. That is why the U−P−PDMS film prepared with ultrafine NaCl templates synthesized by ultrasonic precipitation shows the highest solar reflectivity. As the pore size increases, the scattering efficiency decreases. Specifically, when the size exceeds 100 μm, as observed in the commercial NaCl and cooking salt samples, the pores exhibit minimal scattering of sunlight, which is consistent with the measured solar reflectivity results.

The radiative cooling performance of the U−P−PDMS film was evaluated on the rooftop of a building in Shenzhen, China, under clear sky conditions on a hot day (Figure 4A,B). According to data from the Meteorological Bureau of Shenzhen Municipality, the relative humidity during the testing period was approximately 56%, and the air temperature was recorded at 33.3 °C. However, our recorded rooftop temperature reached approximately 50 °C due to the intense solar heating experienced on the rooftop. We also utilized a light meter (CEM DT-8808) to measure the solar illuminance, showing an intensity of around 100 Klux during the test period (Figure S6). A wood building model was positioned on the rooftop, with a thermocouple placed inside the model. A 5 cm × 5 cm × 1 mm sample of the U−P−PDMS film was applied on top of the building (Figure 4C). For comparison, the temperatures of the bare building model, and the model covered with the C−P−PDMS film produced via cooking salt were also recorded. An infrared (IR) image of the three samples (bare building model, C−P−PDMS covered model, and U−P−PDMS covered model) is presented in Figure 4D, showing that the U−P−PDMS covered model maintains the lowest temperature. As revealed in Figure 4E,F, the average temperature of the U−P−PDMS film was 7 °C lower than the bare model temperature (near the local rooftop temperature), 3 °C lower than the C−P−PDMS covered model in the period of 12:00−13:30. However, cooling performance varies with

https://doi.org/10.1021/acsomega.4c08275
ACS Omega 2025, 10, 1012−1018

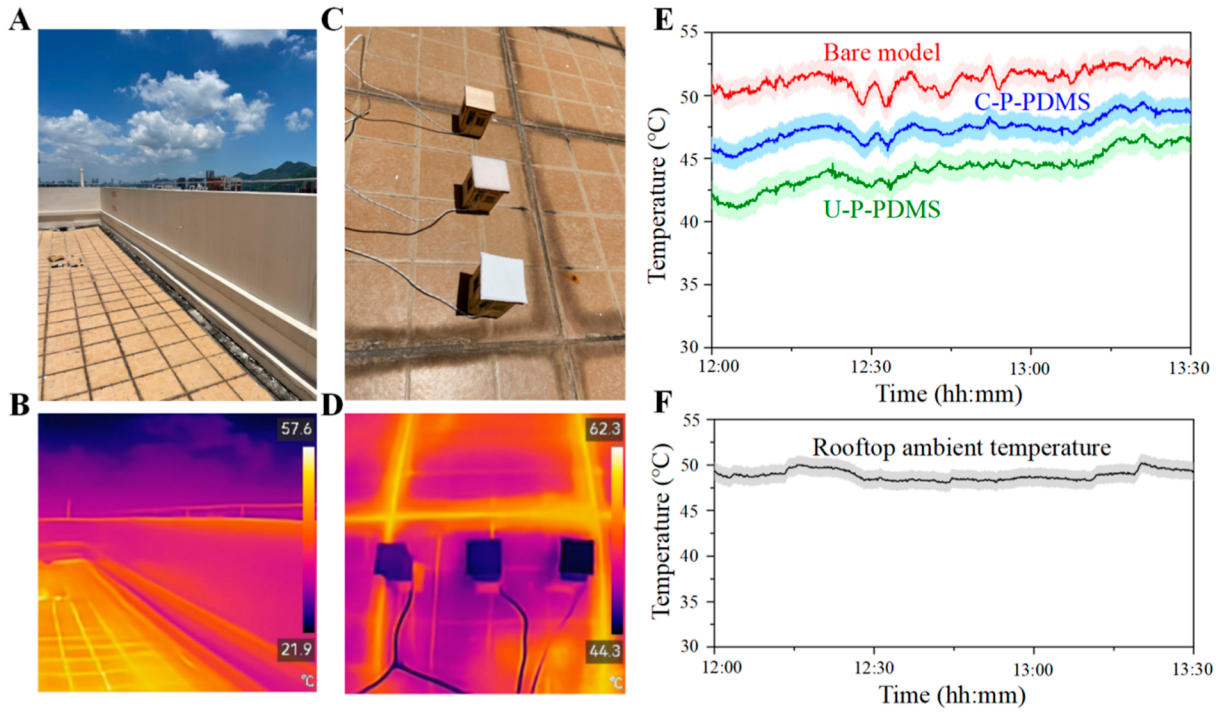

Figure 4. (A) Photograph of the field test rooftop on a clear day. (B) Infrared image of the field test rooftop showing the high ambient temperature (August 03, 2024). (C) Photographs of three building models with a bare building and the other two covered by porous NaCl films (C−P−PDMS and U−P−PDMS). (D) Infrared image of three building models. (E) Real-time temperature curves of the three building models under direct solar irradiation, with error bands (shaded areas) defined by the instrument and measurement error. (F) Real-time monitored ambient temperature, with error bands (shaded areas) defined by the instrument and measurement error.

environmental conditions, that regions with a dry and hot climate tend to have better cooling performance. By comparison, cold, highly humid, or cloudy regions tend to have much lower radiative cooling potentials.[3,36,37] Nevertheless, the results indicated that the U−P−PDMS film, which was fabricated with ultrafine NaCl templates synthesized by ultrasonic precipitation exhibits a superior subambient cooling performance over that fabricated with typically larger NaCl particles.

CONCLUSION

In conclusion, we reported a simple, scalable, and sustainable approach to fabricating porous polymers for radiative cooling. The porous PDMS film was created by employing ultrafine NaCl powders as sacrificial templates, which were synthesized via ultrasonic precipitation to ensure their small size. The ultrafine NaCl powders synthesized through ultrasonic precipitation have a size range centered around 6−8 μm, while those precipitated without sonication are around 40−50 μm. The formation of smaller NaCl crystals was attributed to the influence of ultrasonication on nucleation rate. Compared with larger NaCl templates, the porous PDMS film fabricated with ultrafine NaCl powders shows higher solar reflectivity. This is because reducing the size of NaCl particles decreases pore size, aligning it with the solar spectrum wavelength and enhancing solar scattering efficiency. The as-fabricated porous PDMS film achieves a high thermal emissivity of 0.95 within the atmospheric window (8−13 μm) and exhibits a reflectivity of 0.95 within the visible range (0.4−0.78 μm). Field test shows that the average temperature of the porous PDMS film was 7 °C lower than the local ambient, 3 °C lower than the control PDMS sample fabricated with larger NaCl particles.

ASSOCIATED CONTENT

Supporting Information

The Supporting Information is available free of charge at https://pubs.acs.org/doi/10.1021/acsomega.4c08275.

SEM images of ultrafine NaCl particles synthesized by precipitation under different ultrasonication time; replicated measurement of the solar reflectivity and infrared emissivity of U−P−PDMS; replicated measurement of the solar reflectivity of C−P−PDMS; replicated measurement of the solar reflectivity of M−P−PDMS-5:1; FDTD simulation model for analyzing the scattering efficiency of micropores; a light meter to measure the solar illuminance (PDF)

AUTHOR INFORMATION

Corresponding Authors

Hongmei Zhong − *School of Mechanical and Electrical Engineering, Shenzhen Polytechnic University, Shenzhen, Guangdong 518055, P. R. China;* orcid.org/0009-0006-0983-8485; Email: hmzhong@szpu.edu.cn

Peng Zhang − *CAS Key Laboratory of Mechanical Behavior and Design of Materials, Department of Precision Machinery and Instrumentation, University of Science and Technology of China, Hefei, Anhui 230026, P. R. China;* Email: zhp9036@mail.ustc.edu.cn

Authors

Ting Meng − *CAS Key Laboratory of Mechanical Behavior and Design of Materials, Department of Precision Machinery and Instrumentation, University of Science and Technology of China, Hefei, Anhui 230026, P. R. China*

https://doi.org/10.1021/acsomega.4c08275
ACS Omega 2025, 10, 1012−1018

Wenxiang Ding − *School of Mechanical and Electrical Engineering, Shenzhen Polytechnic University, Shenzhen, Guangdong 518055, P. R. China*
Yi Xiao − *School of Mechanical and Electrical Engineering, Shenzhen Polytechnic University, Shenzhen, Guangdong 518055, P. R. China*

Complete contact information is available at: https://pubs.acs.org/10.1021/acsomega.4c08275

Notes

The authors declare no competing financial interest.

■ ACKNOWLEDGMENTS

We acknowledge the financial support from the National Natural Science Foundation of China (no. 12302251), the Research Project of the Department of Education of Guangdong Province (no. 2022KQNCX227), Shenzhen Science and Technology Innovation Program (nos RCBS20231211090638068, RCBS20231211090550087, 20220812171109001), the Shenzhen Polytechnic Research Funds (nos 6023312015K, 6023312011K).

■ REFERENCES

(1) Henry, A.; Prasher, R.; Majumdar, A. Five thermal energy grand challenges for decarbonization. *Nat. Energy* **2020**, *5* (9), 635−637.
(2) Liang, J.; Wu, J.; Guo, J.; Li, H.; Zhou, X.; Liang, S.; Qiu, C. W.; Tao, G. Radiative cooling for passive thermal management towards sustainable carbon neutrality. *Nat. Sci. Rev.* **2023**, *10* (1), nwac208.
(3) Yin, X.; Yang, R.; Tan, G.; et al. Terrestrial radiative cooling: Using the cold universe as a renewable and sustainable energy source. *Science* **2020**, *370* (6518), 786−791.
(4) Raman, A. P.; Anoma, M. A.; Zhu, L.; et al. Passive radiative cooling below ambient air temperature under direct sunlight. *Nature* **2014**, *515* (7528), 540−544.
(5) Zhai, Y.; Ma, Y.; David, S. N.; et al. Scalable-manufactured randomized glass-polymer hybrid metamaterial for daytime radiative cooling. *Science* **2017**, *355* (6329), 1062−1066.
(6) Zeng, S.; Pian, S.; Su, M.; et al. Hierarchical-morphology metafabric for scalable passive daytime radiative cooling. *Science* **2021**, *373* (6555), 692−696.
(7) Mandal, J.; Fu, Y.; Overvig, A. C.; et al. Hierarchically porous polymer coatings for highly efficient passive daytime radiative cooling. *Science* **2018**, *362* (6412), 315−319.
(8) Chen, M.; Pang, D.; Mandal, J.; et al. Designing mesoporous photonic structures for high-performance passive daytime radiative cooling. *Nano Lett.* **2021**, *21* (3), 1412−1418.
(9) Zhang, Y.; Wang, T.; Mei, X.; et al. Ordered porous polymer films for highly efficient passive daytime radiative cooling. *ACS Photonics* **2023**, *10* (9), 3124−3132.
(10) Zhou, K.; Li, W.; Patel, B. B.; et al. Three-dimensional printable nanoporous polymer matrix composites for daytime radiative cooling. *Nano Lett.* **2021**, *21* (3), 1493−1499.
(11) Zhou, L.; Zhao, J.; Huang, H.; et al. Flexible polymer photonic films with embedded microvoids for high-performance passive daytime radiative cooling. *ACS Photonics* **2021**, *8* (11), 3301−3307.
(12) Li, L.; Liu, G.; Zhang, Q.; et al. Porous structure of polymer films optimized by rationally tuning phase separation for passive all-day radiative cooling. *ACS Appl. Mater. Interfaces* **2024**, *16* (5), 6504−6512.
(13) Song, Y.; Zhan, Y.; Li, Y.; et al. Scalable fabrication of super-elastic TPU membrane with hierarchical pores for subambient daytime radiative cooling. *Sol. Energy* **2023**, *256*, 151−157.
(14) Huang, W.; Chen, Y.; Luo, Y.; Mandal, J.; Li, W.; Chen, M.; Tsai, C.; Shan, Z.; Yu, N.; Yang, Y. Scalable aqueous processing-based passive daytime radiative cooling coatings. *Adv. Funct. Mater.* **2021**, *31* (19), 2010334.
(15) Wang, Y.; Wang, T.; Liang, J.; et al. Controllable-morphology polymer blend photonic metafoam for radiative cooling. *Mater. Horizons* **2023**, *10* (11), 5060−5070.
(16) Ma, J. W.; Zeng, F. R.; Lin, X. C.; et al. A photoluminescent hydrogen-bonded biomass aerogel for sustainable radiative cooling. *Science* **2024**, *385* (6704), 68−74.
(17) Zhang, H.; Ly, K. C. S.; Liu, X.; et al. Biologically inspired flexible photonic films for efficient passive radiative cooling. *Proc. Natl. Acad. Sci.* **2020**, *117* (26), 14657−14666.
(18) Liu, X.; Zhang, M.; Hou, Y.; Pan, Y.; Liu, C.; Shen, C. Hierarchically superhydrophobic stereo-complex poly (lactic acid) aerogel for daytime radiative cooling. *Adv. Funct. Mater.* **2022**, *32* (46), 2207414.
(19) Shan, X.; Liu, L.; Wu, Y.; Yuan, D.; Wang, J.; Zhang, C.; Wang, J. Aerogel-functionalized thermoplastic polyurethane as waterproof, breathable freestanding films and coatings for passive daytime radiative cooling. *Adv. Sci.* **2022**, *9* (20), 2201190.
(20) Wang, X.; Liu, X.; Li, Z.; Zhang, H.; Yang, Z.; Zhou, H.; Fan, T. Scalable flexible hybrid membranes with photonic structures for daytime radiative cooling. *Adv. Funct. Mater.* **2020**, *30* (5), 1907562.
(21) Li, D.; Liu, X.; Li, W.; et al. Scalable and hierarchically designed polymer film as a selective thermal emitter for high-performance all-day radiative cooling. *Nat. Nanotechnol.* **2021**, *16* (2), 153−158.
(22) Liu, J.; Tang, H.; Jiang, C.; Wu, S.; Ye, L.; Zhao, D.; Zhou, Z. Micro-nano porous structure for efficient daytime radiative sky cooling. *Adv. Funct. Mater.* **2022**, *32* (44), 2206962.
(23) Zhou, P.; Wang, Y.; Zhang, X. Supramolecularly Connected Armor-like Nanostructure Enables Mechanically Robust Radiative Cooling Materials. *Nano Lett.* **2024**, *24*, 6395−6402.
(24) Weng, Y.; Zhang, W.; Jiang, Y.; et al. Effective daytime radiative cooling via a template method based PDMS sponge emitter with synergistic thermo-optical activity. *Sol. Energy Mater. Sol. Cell.* **2021**, *230*, 111205.
(25) Zhang, J.; Yang, X.; Xu, R.; et al. An environmentally friendly porous PDMS film via a template method based for passive daytime radiative cooling. *Mater. Lett.* **2024**, *357*, 135686.
(26) Zhou, L.; Rada, J.; Zhang, H.; Song, H.; Mirniaharikandi, S.; Ooi, B. S.; Gan, Q. Sustainable and inexpensive polydimethylsiloxane sponges for daytime radiative cooling. *Adv. Sci.* **2021**, *8* (23), 2102502.
(27) Chen, M.; Pang, D.; Yan, H. Sustainable and self-cleaning bilayer coatings for high-efficiency daytime radiative cooling. *J. Mater. Chem. C* **2022**, *10* (21), 8329−8338.
(28) Hu, Z.; Qiu, Y.; Zhou, J.; Li, Q. Smart flexible porous bilayer for all-day dynamic passive cooling. *Small Sci.* **2024**, *4* (3), 2300237.
(29) Kou, J.; Jurado, Z.; Chen, Z.; et al. Daytime radiative cooling using near-black infrared emitters. *ACS Photonics* **2017**, *4* (3), 626−630.
(30) Nalesso, S.; Bussemaker, M. J.; Sear, R. P.; et al. Development of sodium chloride crystal size during antisolvent crystallization under different sonication modes. *Cryst. Growth Des.* **2019**, *19* (1), 141−149.
(31) Guo, Z.; Zhang, M.; Li, H.; et al. Effect of ultrasound on anti-solvent crystallization process. *J. Cryst. Growth* **2005**, *273* (3−4), 555−563.
(32) Li, H.; Wang, J.; Bao, Y.; et al. Rapid sonocrystallization in the salting-out process. *J. Cryst. Growth* **2003**, *247* (1−2), 192−198.
(33) Lee, J.; Ashokkumar, M.; Kentish, S. E. Influence of mixing and ultrasound frequency on antisolvent crystallisation of sodium chloride. *Ultrason. Sonochem.* **2014**, *21* (1), 60−68.
(34) Wang, T.; Wu, Y.; Shi, L.; Hu, X.; Chen, M.; Wu, L. A structural polymer for highly efficient all-day passive radiative cooling. *Nat. Commun.* **2021**, *12* (1), 365.
(35) Liu, J.; Wei, Y.; Zhong, Y.; Zhang, L.; Wang, B.; Feng, X.; Xu, H.; Mao, Z. Hierarchical Gradient Structural Porous Metamaterial with Selective Spectral Response for Daytime Passive Radiative Cooling. *Adv. Funct. Mater.* **2024**, *34*, 2406393.

(36) Liu, C.; Wu, Y.; Wang, B.; et al. Effect of atmospheric water vapor on radiative cooling performance of different surfaces. *Sol. Energy* **2019**, *183*, 218−225.
(37) Gao, Y.; Song, X.; Farooq, A. S.; et al. Cooling performance of porous polymer radiative coating under different environmental conditions throughout all-year. *Sol. Energy* **2021**, *228*, 474−485.

https://doi.org/10.1021/acsomega.4c08275
ACS Omega 2025, 10, 1012−1018